MedScience
https://doi.org/10.1007/s11684-026-1237-8

RESEARCH ARTICLE

PDRG1 induced by SP1 facilitates the proliferation and metastasis of hepatocellular carcinoma by activating the Wnt/β-catenin pathway

Xudong Zhao[1,2,*], Shihua Lv[11,12,*], Haikuan Wang[1], Zeyi Lu[1], Pengcheng Kang[1], Jinglin Li[1], Liang Yu[1], Shihui Ma[1], Changxing Hua[1], Junqi You[1], Ziqiang Ge[1], Yi Xu (✉)[1,3,4,5,6,7,8,9,10], Yunfu Cui (✉)[1]

[1]Department of Hepatopancreatobiliary Surgery, The Second Affiliated Hospital of Harbin Medical University, Harbin 150086, China; [2]Future Medical Laboratory, The Second Affiliated Hospital of Harbin Medical University, Harbin 150086, China; [3]State Key Laboratory of Oncology in South China, Cancer Center of Sun Yat-sen University, Guangzhou 510000, China; [4]Shanghai Key Laboratory of Cancer Systems Regulation and Clinical Translation, Jiading District Central Hospital Affiliated to Shanghai University of Medicine & Health Science, Shanghai 201800, China; [5]Key Laboratory of Clinical Laboratory Technology for Precision Medicine (Fujian Medical University), Fujian Province University, Fuzhou 350000, China; [6]Key Laboratory of Early Prevention and Treatment for Regional High Frequency Tumor (Guangxi Medical University), Ministry of Education/Guangxi Key Laboratory of Early Prevention and Treatment for Regional High Frequency Tumor, Nanning 530000, China; [7]Key Laboratory of Clinical Laboratory Medicine of Guangxi Department of Education, Nanning 530000, China; [8]Key Laboratory of Gastrointestinal Cancer (Fujian Medical University), Ministry of Education, School of Basic Medical Sciences, Fujian Medical University, Fuzhou 350122, China; [9]Department of Pathology, Li Ka Shing Faculty of Medicine, The University of Hong Kong, Hong Kong SAR 999077, China; [10]Materials Innovation Institute for Life Sciences and Energy (MILES), HKU-SIRI, Shenzhen 518000, China; [11]State Key Laboratory of Frigid Zone Cardiovascular Diseases, Harbin 150081, China; [12]Department of Anesthesiology, Harbin Medical University Cancer Hospital, Harbin 150081, China

Abstract **Hepatocellular carcinoma (HCC) remains a lethal malignancy with limited therapeutic targets. P53 and DNA damage-regulated gene 1 (PDRG1) has emerged as an oncogene in multiple cancers, yet its role and regulatory mechanism in HCC remain unclear. Here, we demonstrated that PDRG1 expression was significantly upregulated in HCC tissues compared to normal liver, correlating with advanced tumor stage, higher grade, and poor patient survival. Functionally, PDRG1 knockdown suppressed HCC cell proliferation, migration, and invasion *in vitro* and inhibited tumor growth and lung metastasis *in vivo*, whereas PDRG1 overexpression exerted opposite effects. Mechanistically, PDRG1 activated Wnt/β-catenin signaling, elevating levels of β-catenin, c-Myc, and phosphorylated GSK-3β, and the oncogenic effects of PDRG1 were reversed by the Wnt pathway inhibitor XAV939. Furthermore, transcription factor Specificity Protein 1 (SP1) bound directly to the PDRG1 promoter at the E3 site (−1927 to −1917) and activated its transcription. The pro-tumor effects of SP1 were rescued by PDRG1 silencing, indicating that SP1 acts through PDRG1. Collectively, our study identifies SP1 as an upstream transcriptional activator of PDRG1 and defines the SP1/PDRG1/Wnt/β-catenin axis as a key regulatory pathway promoting HCC progression, suggesting its potential as a prognostic biomarker and therapeutic target.**

Keywords hepatocellular carcinoma; PDRG1; Wnt/β-catenin signaling; transcriptional regulation; prognostic biomarker

Introduction

Hepatocellular carcinoma (HCC) ranks among the most prevalent malignancies of the digestive system worldwide. Characterized by insidious onset, high rates of recurrence and metastasis, HCC significantly impacts patient prognosis. Currently, it stands as the third leading cause of cancer-related mortality globally [1]. Although significant advancements have been made in HCC treatment, a considerable proportion of patients are diagnosed at an advanced stage during their initial presentation due to the lack of prominent clinical symptoms. Furthermore, the propensity for early metastasis and rapid recurrence contributes to the dismal prognosis associated with this disease [2,3]. To date, the precise pathogenesis of HCC

Received July 28, 2025; accepted January 29, 2026
Correspondence: Yi Xu, xuyihrb@pathology.hku.hk;
Yunfu Cui, yfcui7@163.com

*These authors contributed equally to this work.

remains incompletely elucidated. Existing research indicates that factors such as alcohol consumption, non-alcoholic fatty liver disease (NAFLD), viral hepatitis, consumption of mold-contaminated food, and genetic predisposition can all contribute to HCC development [4]. Therefore, elucidating the molecular mechanisms underlying HCC pathogenesis and identifying effective therapeutic targets are of paramount importance for improving patient outcomes.

P53 and DNA damage-regulated gene 1 (PDRG1), located on chromosome 20q13.12, encodes a small protein of 133 amino acids (13.6 kDa). Luo *et al*. first identified in 2003 that PDRG1 expression is regulated by ultraviolet (UV) radiation and the tumor suppressor p53 [5]. Furthermore, PDRG1 is implicated in various cellular physiologic processes, including cell proliferation, growth, apoptosis, cell cycle regulation, and DNA damage repair [6]. Recent studies have revealed that PDRG1 expression is significantly elevated in multiple tumor types, including colorectal, ovarian, lung, gastric, breast, and uterine cancers, compared to adjacent normal tissues. Consequently, PDRG1 has been proposed as a novel tumor biomarker. Mechanistically, Xu *et al*. demonstrated that PDRG1 participates in the malignant progression of colorectal cancer by modulating the p21-mediated signaling pathway [7]. Zhang *et al*. reported that PDRG1 silencing suppresses the growth and metastasis of gastric cancer cells via activation of the ataxia–telangiectasia mutated (ATM)/p53 pathway [8]. Additionally, PDRG1 silencing has been shown to inhibit the Wnt signaling pathway in esophageal cancer cells [9]. However, the expression profile of PDRG1 in HCC and its precise mechanistic role in regulating HCC cell behavior remain incompletely understood.

The Wnt/β-catenin pathway, a canonical Wnt signaling cascade, regulates diverse biological processes including proliferation, apoptosis, migration, and invasion [10]. Recent research indicates that aberrant Wnt/β-catenin signaling is prevalent in numerous malignancies and exerts significant clinical impacts on tumor biology, patient prognosis, and therapeutic response [11,12]. In the absence of Wnt ligand activation, the destruction complex—comprising Axin, adenomatous polyposis coli (APC), and GSK3β proteins—binds and phosphorylates β-catenin, targeting it for ubiquitin-mediated degradation and preventing its cytoplasmic accumulation under physiologic conditions [13]. Upon Wnt pathway activation, binding of Wnt ligands to frizzled receptors (FZDs) on the cell membrane activates dishevelled (Dvl) protein. This inhibits the destruction complex, allowing non-phosphorylated β-catenin to accumulate in the cytoplasm. Subsequently, non-phosphorylated β-catenin translocates to the nucleus, where it associates with transcription factors of the T cell factor/lymphoid enhancer factor (TCF/LEF) family, initiating transcription of Wnt-regulated target genes such as c-Myc [14,15].

Specificity protein 1 (SP1), a sequence-specific DNA binding protein, has been documented in early studies to exhibit dysregulated expression and activation in tumor tissues [16]. As a prominent member of the transcription factor family, SP1 activates the transcription of numerous cellular genes harboring GC-rich binding sites within their promoters [17]. During tumor progression across various cancers, SP1 can transactivate numerous oncogenes while simultaneously suppressing certain tumor suppressor genes [18]. Multiple studies demonstrate the involvement of SP1 in regulating tumor cell proliferation, invasion, angiogenesis, and other biological functions. Furthermore, its expression level in tumor tissues correlates with patient prognosis and treatment outcomes [19,20].

In the present study, we demonstrate that PDRG1 is overexpressed in HCC tissues, correlating with poor prognosis in HCC patients. Inhibition of PDRG1 suppresses tumor formation, proliferation, and invasion by modulating the Wnt/β-catenin pathway. Furthermore, we identify PDRG1 as a direct downstream transcriptional target of SP1. Critically, knockdown of PDRG1 reverses the tumor-promoting functions induced by SP1 overexpression. Collectively, our findings establish that the SP1/PDRG1/Wnt/β-catenin axis regulates HCC tumorigenesis and progression. These results highlight PDRG1 as a potential therapeutic target for developing novel treatment strategies against HCC.

Materials and methods

Public data analysis

The expression levels of PDRG1 and SP1 in HCC versus normal liver tissues were analyzed using the UALCAN web portal and the Gene Expression Omnibus (GEO). UALCAN employs Level 3 standardized data from The Cancer Genome Atlas (TCGA) and Clinical Proteomic Tumor Analysis Consortium (CPTAC) databases. For CPTAC, protein expression Z-values represent standard deviations from the median across samples, based on $\log_2$ spectral count ratios normalized within and across samples. Correlations between PDRG1 expression and tumor stage/grade in TCGA were evaluated using Welch's *t*-test. Survival analysis was performed using the GepLiver platform with the TCGA-LIHC cohort. Kaplan–Meier curves were generated and compared by the log-rank test, with patients stratified according to the median expression level of PDRG1. This analytical approach aligns with standard bioinformatic methodologies for cancer prognosis studies using TCGA data, with a significance threshold of $P < 0.05$. The GEPIA2 portal was used to analyze correlations between PDRG1 and selected genes in the TCGA-LIHC data set. Expression

values were log_2-transformed, and Pearson correlation analysis was applied, reporting the correlation coefficient (R) and *P*-value. A significance threshold of $P < 0.05$ was applied to all analyses. Detailed information on all data sets used in this study is provided in Table S1.

Gene set enrichment analysis (GSEA)

GSEA was performed using GSEA software (version 3.0). Samples were stratified into PDRG1 high-expression (⩾ 50%) and low-expression (< 50%) groups based on PDRG1 expression levels. The h.all.v7.4.symbols.gmt gene set was acquired from the Molecular Signatures Database for pathway enrichment analysis. The analysis parameters were set as follows: minimum gene set size = 5, maximum gene set size = 5000, with 1000 permutations. A nominal *P*-value < 0.05 was considered statistically significant.

Protein–protein interaction (PPI) network analysis

The PPI network of PDRG1 was constructed using the STRING database (version 12.0). The search was performed with PDRG1 as the query protein in Homo sapiens, requiring an interaction score > 0.7 (high confidence). The resulting network included both known and predicted interactions, covering physical associations and functional linkages. The network graph was exported and further visualized using Cytoscape software (version 3.9.1).

Clinical specimens

Sixty-six pairs of tumor tissues and matched adjacent non-tumorous tissues (collected 2 cm from the tumor margin) were obtained from patients undergoing hepatectomy at the Department of Hepatobiliary and Pancreatic Surgery, The Second Affiliated Hospital of Harbin Medical University (Harbin, China) between May 2024 and June 2025. All diagnoses were pathologically confirmed postoperatively. Inclusion criteria were: (1) Child-Pugh class A or B; (2) No prior antitumor therapy; (3) R0 radical resection; (4) Postoperative pathological diagnosis of HCC; (5) Availability of microvascular invasion (MVI) description in the pathology report. Exclusion criteria included: (1) Recurrent HCC; (2) Extrahepatic metastasis; (3) Previous history of malignancy; (4) Presence of portal/hepatic vein tumor thrombus; (5) History of immunomodulatory drug use. All specimens were immediately snap-frozen in liquid nitrogen and stored at 80 °C. Informed consent was obtained from all participants, and the study protocol was approved by the Institutional Review Board (IRB) of The Second Affiliated Hospital of Harbin Medical University (Approval No. YSJKY2024-235).

Immunohistochemical (IHC) analysis

IHC staining for PDRG1 protein expression was performed on a subset of 30 HCC cases randomly selected from the 66 cases collected between May 2024 and June 2025 at The Second Affiliated Hospital of Harbin Medical University. IHC staining intensity was evaluated using a semiquantitative scoring system based on the percentage of strongly stained cells within the observed field. The association between PDRG1 expression levels in HCC tumors and adjacent tissues was determined using the paired samples *t*-test.

Cell culture

The HCC cell lines HCCLM3, Huh7, MHCC97-H, and Hep3B were obtained from the Cell Bank of the Chinese Academy of Sciences (Shanghai, China). The PLC/PRF/5 cell line was purchased from the American Type Culture Collection (ATCC). Cells were cultured in Dulbecco's Modified Eagle Medium (DMEM) (Gibco) supplemented with 10% fetal bovine serum (FBS) (Abcells) and 1% Penicillin-Streptomycin Solution (Seven). All cells were maintained in a humidified incubator at 37 °C with 5% CO_2. The Wnt/β-catenin pathway-specific inhibitor XAV939 was purchased from MedChemExpress (USA) and used to treat relevant HCC cells at a concentration of 3.5 μmol/L.

Plasmids, lentivirus, and siRNA transfection

Lentiviruses encoding short hairpin RNAs (shRNAs) targeting PDRG1 (shPDRG1-1) or a non-targeting control (shNT) sequence were purchased from Shanghai Nobio Biotechnology Co., Ltd. (China). Lentiviruses co-expressing luciferase (Luc) with either OE-PDRG1 or empty vector (Vector) were obtained from Wuhan GeneCreate Biological Engineering Co., Ltd. (China). Small interfering RNAs (siRNAs) targeting PDRG1 (si-PDRG1-1 and si-PDRG1-2), and plasmids containing the empty vector, full-length PDRG1 cDNA (OE-PDRG1), or full-length SP1 cDNA (OE-SP1) were purchased from Wuhan GeneCreate Biological Engineering Co., Ltd. (China). For lentiviral infection, HCC cells were incubated overnight with virus-containing supernatant supplemented with 8 μg/mL Polybrene®. Plasmid and siRNA transfection was performed using the Lipofectamine™ 3000 Transfection Reagent (Thermo Fisher Scientific, Waltham, MA, USA) according to the manufacturer's instructions; complexes were formed by incubating the nucleic acid with the reagent for 20 min before addition to the cell culture medium. Cells were subjected to gain-of-function or loss-of-function experiments 72 h post-infection/transfection.

Cell counting kit-8 (CCK-8) assay

HCC cells seeded in 96-well plates were incubated with 10 μL of CCK-8 solution (Sevenbio, Beijing, China) per well for 2 h at 37 °C. The optical density (OD) at 450 nm was measured using a Synergy HTX Multi-Mode Microplate Reader (BioTek Instruments, Inc., Winooski, VT, USA).

Colony formation assay

HCC cells were plated in 6-well plates at a density of 800 cells per well and cultured for 14 days under standard conditions (37 °C, 5% CO_2). Resulting colonies were fixed with 4% paraformaldehyde for 15 min, washed twice with phosphate-buffered saline (PBS), and stained with 1 mL of 0.1% crystal violet solution (Beyotime, Shanghai, China) for 20 min. After washing and air-drying, colonies (defined as clusters > 50 cells) were counted manually or using ImageJ software (National Institutes of Health, Bethesda, MD, USA).

Wound healing assay

HCC cells were seeded in 6-well plates and cultured to form a confluent monolayer. A straight scratch wound was created across the monolayer using a sterile 200-μL pipette tip, guided by a straightedge. The wells were gently washed three times with PBS to remove detached cells and debris, and serum-free DMEM was added. Initial images (0 h) of the wound were captured using phase-contrast microscopy. After 48 h of incubation, the wells were washed gently with PBS, and final images were captured. Wound closure percentage was quantified by comparing the remaining wound area at 48 h to the initial wound area at 0 h using ImageJ software.

Transwell migration assay

Cell migration was assessed using Transwell chambers (8.0-μm pore size, Corning Inc., Corning, NY, USA). Briefly, 5×10^4 HCC cells resuspended in 200 μL of serum-free DMEM were seeded into the upper chamber. The lower chamber was filled with 600 μL of DMEM containing 10% FBS as a chemoattractant. After incubation for 48 h at 37 °C with 5% CO_2, non-migrated cells on the upper surface of the membrane were gently removed with a cotton swab. Cells that had migrated to the lower surface were fixed with 4% paraformaldehyde for 15–20 min, stained with 0.1% crystal violet solution for 20–40 min (with intermittent PBS washes), and air-dried. Migrated cells were photographed using an inverted microscope and quantified by counting cells in three random fields per chamber.

Transwell invasion assay

Transwell invasion assays were performed using chambers pre-coated with Matrigel® Matrix (Corning Inc., Corning, NY, USA). Briefly, Matrigel® was thawed at 4 °C, diluted 1:3 with ice-cold serum-free DMEM, and 100 μL of the mixture was added to the upper chamber of a Transwell insert (8.0-μm pore size) placed in a 24-well plate, ensuring even coverage of the membrane. The plate was incubated at 37 °C for 4 h to allow gel polymerization. Excess liquid was then carefully aspirated. 1×10^5 HCC cells suspended in 200 μL of serum-free DMEM were seeded onto the solidified Matrigel® layer in the upper chamber. The lower chamber was filled with 600 μL of DMEM supplemented with 10% FBS as a chemoattractant. After 48 h of incubation at 37 °C with 5% CO_2, non-invading cells on the upper surface of the membrane were removed with a cotton swab. Cells that had invaded through the Matrigel® and membrane to the lower surface were fixed with 4% paraformaldehyde for 15–20 min, stained with 0.1% crystal violet solution for 40 min (with three washes in PBS during staining), and air-dried. Invaded cells were photographed using an inverted microscope and quantified by counting cells in three randomly selected fields per membrane.

Reverse transcription-quantitative polymerase chain reaction (RT-qPCR)

Total RNA was extracted from HCC cell lines and clinical tissue specimens (paired tumor and adjacent normal tissues) using the Sevenfast® Total RNA Extraction Kit (Sevenbio, Beijing, China). For tissue samples, approximately 30 mg of each specimen was homogenized prior to RNA extraction. RNA concentration and purity were verified spectrophotometrically. Then, 1000 ng of total RNA was reverse transcribed into cDNA using the All-in-one First Strand cDNA Synthesis Kit II (with dsDNase) (Sevenbio). Quantitative PCR was performed with 2× SYBR Green qPCR MasterMixII (Universal) (Sevenbio) on a QuantStudio™ Real-Time PCR System (Thermo Fisher Scientific). Glyceraldehyde-3-phosphate dehydrogenase (GAPDH) was used as the internal control, and relative expression levels were calculated by the $2^{-\Delta\Delta Ct}$ method. All human tissues were obtained with informed consent, and the study was approved by the Institutional Review Board of The Second Affiliated Hospital of Harbin Medical University (Approval No. YSJKY2024-235). The primer sequences used were:

PDRG1: Forward 5′-ATTGTGGACCTGGACACTAA-AAGG-3′, Reverse 5′-TGTCTCAGGGTGAGGCATCT-TG-3′

SP1: Forward 5′-CACCAGAATAAGAAGGGAGG-3′,

Reverse 5′-GGTGGTAATAAGGGCTGAA-3′

GAPDH: Forward 5′-GGTGTGAACCATGAGAAG-TATGA-3′, Reverse 5′-GAGTCCTTCCACGATACCA-AAG-3′

PDRG1 promoter E1 region: Forward 5′-CGCCTT-TTACAGCCATGTGG-3′, Reverse 5′-AACAGCCAGC-GTATGTGGAA-3′

PDRG1 promoter E2 region: Forward 5′-TAGTGTTA-GAGCCTGCGCAC-3′, Reverse 5′-GATAGCATAGCG-CCCACCAA-3′

PDRG1 promoter E3 region: Forward 5′-TGTGTTC-ACTGCTGCATCCT-3′, Reverse 5′-CTGCCTCTGACC-CGTTACTC-3′

Western blot

Total protein was extracted from cells or tissues using RIPA lysis buffer supplemented with protease and phosphatase inhibitors (Beyotime, Shanghai, China). Protein concentration was determined using the BCA Protein Assay Kit (Beyotime). Equal amounts of protein (30 μg) were separated by SDS-polyacrylamide gel electrophoresis (SDS-PAGE) and transferred onto PVDF membranes. Membranes were blocked with 5% non-fat milk in Tris-buffered saline containing 0.1% Tween-20 (TBST) for 1 h at room temperature and then incubated with primary antibodies diluted in blocking buffer overnight at 4 °C. After washing three times with TBST, membranes were incubated with appropriate horseradish peroxidase (HRP)-conjugated secondary antibodies for 50 min at room temperature. Following three additional TBST washes, protein bands were visualized using enhanced chemiluminescence (ECL) substrate (Beyotime) and imaged using a Bio-Rad ChemiDoc Touch Imaging System (Bio-Rad Laboratories, Hercules, CA, USA). Band intensity was quantified using ImageJ software (National Institutes of Health).

Co-immunoprecipitation (Co-IP) assay

PPI between RUVBL1 and PDRG1 was analyzed by co-immunoprecipitation using the Pierce™ Magnetic Direct Co-IP Kit (Thermo Fisher Scientific, Cat# 88828). Total proteins were extracted from Hep3B and PLC/PRF/5 cells using IP Lysis/Wash Buffer with protease inhibitors. Cell lysates were diluted to 2 mg/mL with the same buffer. For each reaction, 5 μg of antibody—anti-RUVBL1 (Proteintech, Cat# 10210-2-AP), anti-PDRG1 (Santa Cruz Biotechnology, Cat# sc-398815), or normal rabbit IgG (Proteintech, Cat# 30000-0-AP, as a negative control)—was cross-linked to magnetic beads. Then, 500 μL of diluted lysate was added to the antibody-conjugated beads and incubated overnight at 4 °C. After washing, bound proteins were eluted and analyzed by Western blot.

Nuclear protein extraction

Nuclear and cytoplasmic fractions were isolated using the Nuclear and Cytoplasmic Protein Extraction Kit (Beyotime, Shanghai, China) strictly following the manufacturer's instructions. Histone H3 (H3) was used as a nuclear fraction loading control.

Chromatin immunoprecipitation (ChIP)

ChIP assays were performed using the SimpleChIP® Enzymatic Chromatin IP Kit (Cell Signaling Technology, Danvers, MA, USA; #9005S). Briefly, cells were cross-linked with 37% formaldehyde for 10 min at room temperature, and the reaction was quenched by adding 125 mmol/L glycine for 5 min. Cells were washed with ice-cold PBS, harvested, and lysed. Chromatin was digested with Micrococcal Nuclease to obtain DNA fragments predominantly between 150 bp and 900 bp. Chromatin was immunoprecipitated overnight at 4 °C with rotation using anti-SP1 antibody (CST #9389S) or normal rabbit IgG as a negative control. Protein G Magnetic Beads were added for 2 h to capture the antibody-chromatin complexes. Complexes were washed sequentially with low salt, high salt, LiCl, and TE buffers. Cross-links were reversed by incubation with 200 mmol/L NaCl at 65 °C for 30 min, followed by proteinase K digestion. Immunoprecipitated DNA was purified using spin columns. Enrichment of specific DNA fragments was analyzed by qPCR using primers targeting the predicted binding sites (E1, E2, E3) within the PDRG1 promoter region (sequences listed above).

Luciferase reporter assay

The pmirGLO vector containing the PDRG1 promoter region was purchased from Wuhan GeneCreate Biological Engineering Co., Ltd. (China). HCC cells were co-transfected with the PDRG1-promoter reporter construct and either OE-SP1 plasmid or empty vector control using Lipofectamine™ 3000. Renilla luciferase plasmid (pRL-TK) was co-transfected as an internal control for normalization. Forty-eight hours post-transfection, luciferase activity was measured using the Dual-Luciferase® Reporter Assay System (Vazyme Biotech Co., Ltd., Nanjing, China) according to the manufacturer's instructions. Firefly luciferase activity was normalized to Renilla luciferase activity for each sample.

***In vivo* tumorigenesis and metastasis assay**

All procedures were approved by the Institutional Animal Care and Use Committee (IACUC) of The Second Affiliated Hospital of Harbin Medical University

(Approval No. YSJKY2024-235).

Subcutaneous tumor model

Six-week-old male BALB/c nude mice (SPF conditions) received subcutaneous injections of Hep3B cells stably transduced with lentivirus encoding shNT or shPDRG1-1. Cells (1×10^6) were resuspended in 100 μL of sterile PBS and injected into the left flank of each mouse ($n = 6$ per group). Tumor volume was measured every three days using the formula: Volume = $0.5 \times \text{length} \times \text{width}^2$. Mice were euthanized at four weeks, and tumors were collected for analysis.

Lung metastasis model

Hep3B cells stably transduced with lentivirus co-expressing luciferase (Luc) and OE-PDRG1 or empty vector (Vector) were injected via tail vein (1×10^6 cells in 100 μL PBS) into male BALB/c nude mice. Mice were divided into four groups ($n = 6$/group): Vector + PBS, Vector + XAV939, OE-PDRG1 + PBS, and OE-PDRG1 + XAV939. XAV939 was prepared from a 100 mmol/L DMSO stock solution and diluted to a final concentration of 10 mg/mL (DMSO ⩽ 0.1%). Mice in the XAV939 groups received intraperitoneal injections (10 mg/kg) every other day for 6 weeks, while control groups received PBS. At six weeks post-injection, all mice underwent bioluminescence imaging using an IVIS Lumina XRMS system (PerkinElmer) and were subsequently euthanized for lung tissue collection and further analysis.

Statistical analysis

All statistical analyses and graphing were performed using GraphPad Prism software (version 9.5.1) and SPSS Statistics (version 22.0). Quantitative data are presented as the mean ± standard deviation (SD). Comparisons between two groups were performed using Student's *t*-test. Comparisons among multiple groups were analyzed using one-way analysis of variance (ANOVA) followed by Tukey's post-hoc test. The association between PDRG1 expression and clinicopathological parameters was assessed using the Chi-square test or Fisher's exact test, as appropriate. All cell-based experiments were independently repeated at least three times. A $P < 0.05$ was considered statistically significant.

Results

Elevated PDRG1 predicts poor prognosis in HCC

Analysis of The Cancer Genome Atlas (TCGA) and Gene Expression Omnibus (GEO) data sets using the UALCAN platform revealed that PDRG1 mRNA expression was significantly higher in HCC tissues compared to normal liver tissues ($P < 0.0001$, Fig. 1A and 1B). Further analysis of the relationship between PDRG1 expression and specific etiological factors showed that among alcohol consumption, non-alcoholic fatty liver disease (NAFLD), hepatitis B, and hepatitis C, only NAFLD demonstrated a significant inverse association with PDRG1 expression ($P < 0.05$), while the other three factors showed no statistically significant association (Fig. S1A). Furthermore, data from the Clinical Proteomic Tumor Analysis Consortium (CPTAC) demonstrated upregulation of PDRG1 protein in HCC tissues versus normal liver controls ($P < 0.0001$, Fig. 1C). Validation using our clinical specimens ($n = 66$ pairs) via Western blot, immunohistochemistry (IHC), and RT-qPCR consistently confirmed that PDRG1 expression was significantly elevated in HCC tissues at both protein and mRNA levels compared to matched adjacent non-tumorous tissues ($P < 0.0001$, Fig. 1D–1F).

PDRG1 mRNA expression increased progressively with higher tumor grade, a trend that was statistically significant. However, such a consistent increase was not observed across pathological tumor stages (stage I–IV) ($P < 0.05$, Fig. 2A and 2B). Analysis of our cohort, in which patients were stratified into high- and low-expression groups based on the median PDRG1 protein level, further established significant associations between elevated PDRG1 expression and key clinicopathological parameters, including tumor number, capsular invasion, tumor diameter, and MVI ($P < 0.05$, Table 1). The relationship between PDRG1 expression levels and these statistically significant parameters was further visualized using box plots with overlaid scatter points. ($P < 0.05$, Fig. S1B). Critically, analysis of TCGA data via the GepLiver platform demonstrated that HCC patients with high PDRG1 mRNA expression had significantly worse survival outcomes. This included reduced overall survival (OS), disease-specific survival (DSS), disease-free survival (DFS), and progression-free survival (PFS) ($P < 0.05$ for all, Fig. 2C–2F). Collectively, these results indicate that PDRG1 is a potential biomarker predictive of poor prognosis in HCC.

PDRG1 facilitates HCC cell proliferation, migration, and invasion

Analysis of five HCC cell lines (Huh7, HCCLM3, Hep3B, MHCC97-H, and PLC/PRF/5) via Western blot and RT-qPCR revealed significantly higher levels of both PDRG1 protein and mRNA in Hep3B and PLC/PRF/5 cells, while HCCLM3 cells exhibited the lowest expression (Fig. 3A and 3B). Transfection of Hep3B and PLC/PRF/5 cells with two distinct PDRG1-targeting

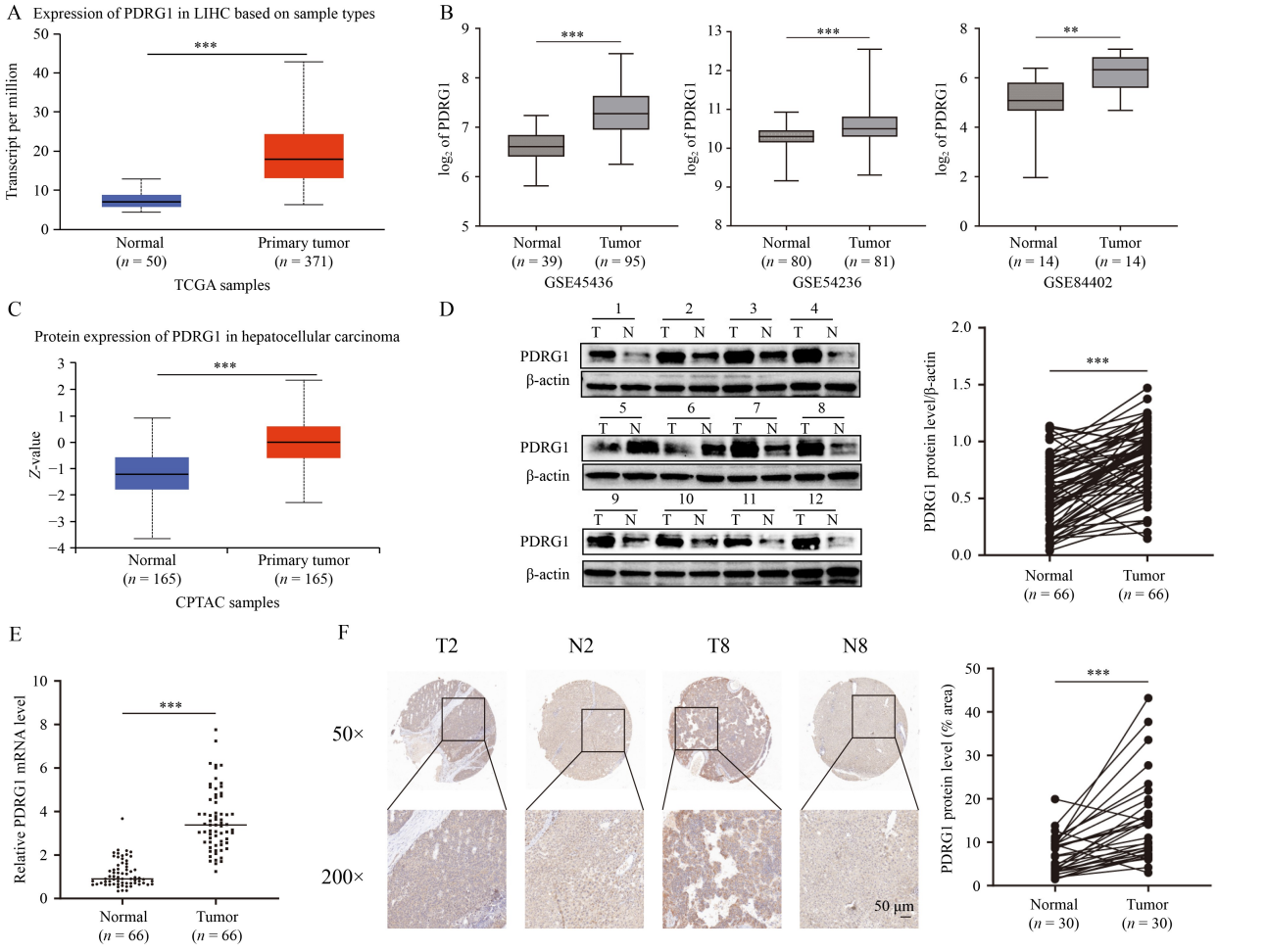

Fig. 1 Expression of PDRG1 in HCC. (A) Differential expression of PDRG1 mRNA between HCC and normal liver tissues in the TCGA database analyzed by UALCAN platform. (B) PDRG1 mRNA expression in HCC versus normal liver tissues from the GEO database. (C) PDRG1 protein expression in HCC compared to normal liver tissues from the CPTAC database, analyzed via UALCAN. (D) Western blot analysis of PDRG1 protein in 66 paired normal and tumor tissues. (E) RT-qPCR detection of PDRG1 mRNA in 66 paired normal and tumor specimens. (F) Immunohistochemical (IHC) staining of PDRG1 protein in 30 paired normal and tumor tissues, with representative images at 50× and 200× magnification. CPTAC, Clinical Proteomic Tumor Analysis Consortium; HCC, hepatocellular carcinoma; LIHC, liver hepatocellular carcinoma; PDRG1, P53 and DNA damage-regulated gene 1; TCGA, The Cancer Genome Atlas. *$P < 0.05$, **$P < 0.01$, ***$P < 0.001$.

siRNAs (si-PDRG1-1 and si-PDRG1-2) significantly downregulated PDRG1 expression at both mRNA and protein levels ($P < 0.0001$, Fig. 3C–3F). Conversely, overexpression of PDRG1 (OE-PDRG1) in HCCLM3 cells markedly elevated PDRG1 mRNA and protein levels ($P < 0.001$, Fig. 3G and 3H).

Functional assays demonstrated that PDRG1 knockdown significantly inhibited HCC cell proliferation, as evidenced by CCK-8 and colony formation assays ($P < 0.05$, Fig. 3I–3M). Overexpression of PDRG1 significantly enhanced proliferation (Fig. 3I–3M). Furthermore, PDRG1 knockdown significantly attenuated HCC cell migration and invasion in wound healing and Transwell assays, while PDRG1 overexpression markedly promoted both processes ($P < 0.01$, Fig. 3N and 3O). Collectively, these data establish PDRG1 as an oncogene in HCC.

PDRG1 regulates the Wnt/β-Catenin pathway

Analysis of 374 HCC patients from the TCGA database, stratified by median PDRG1 expression into high- and low-expression groups, identified differentially expressed genes (DEGs) (Fig. 4A and 4B). KEGG pathway analysis showed significant enrichment of DEGs in Spliceosome, RNA transport, and Ubiquitin-mediated proteolysis (Fig. 4C). Gene Ontology (GO) enrichment analysis of DEGs revealed significant enrichment in: biological process (BP): RNA splicing and mRNA metabolic process (Fig. 4D); cellular component (CC): nucleoplasm and nuclear part (Fig. 4E); molecular function (MF): RNA binding, nucleic acid binding, and chromatin binding (Fig. 4F).

GSEA indicated that PDRG1 expression was

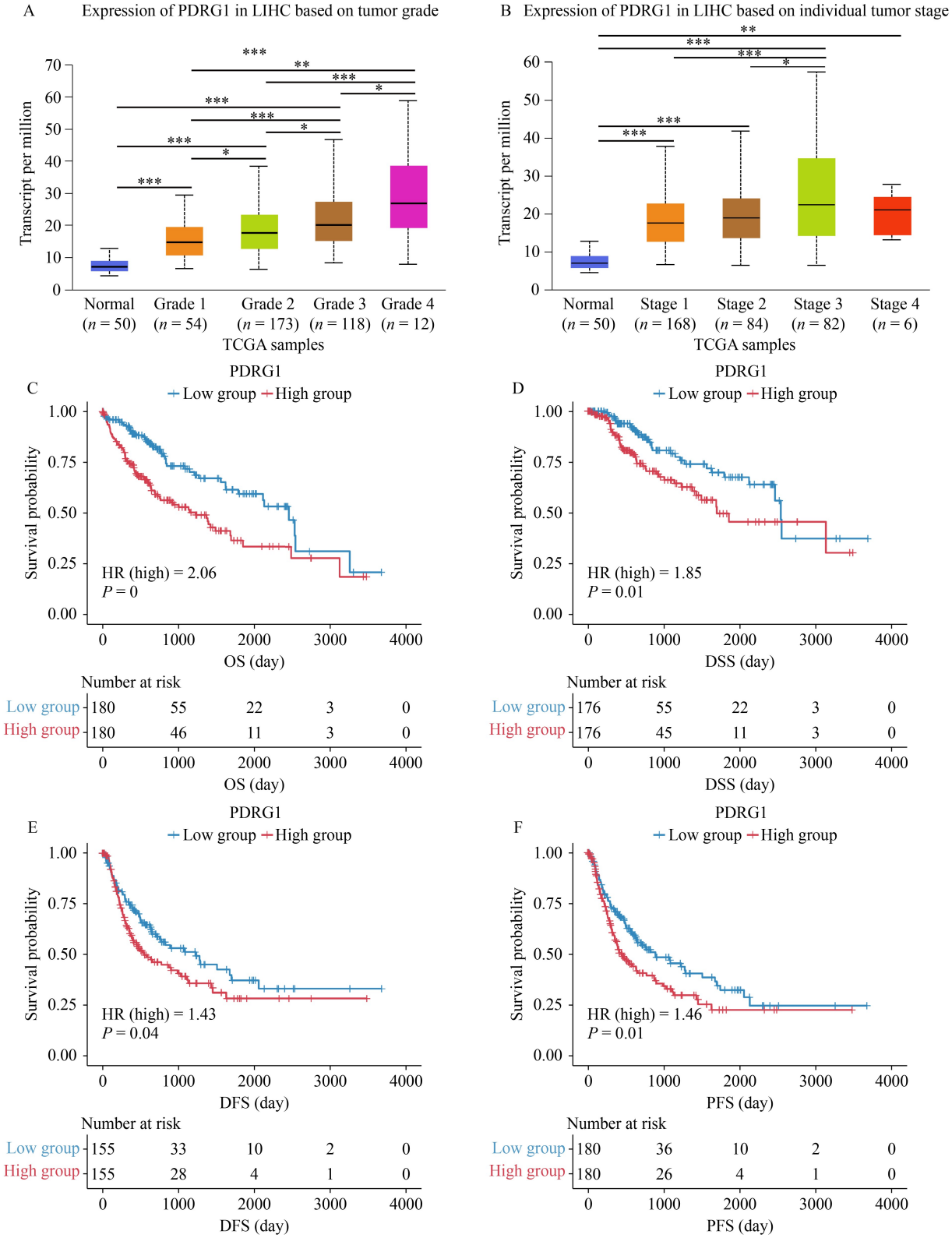

Fig. 2 Clinical significance of PDRG1 expression in hepatocellular carcinoma (HCC). (A) PDRG1 mRNA expression across tumor grade in TCGA analyzed by UALCAN. (B) PDRG1 mRNA expression by tumor stage in TCGA via UALCAN. (C–F) Survival analysis using GepLiver based on PDRG1 expression in TCGA. DFS, disease-free survival; DSS, disease-specific survival; HCC, hepatocellular carcinoma; LIHC, liver hepatocellular carcinoma; OS, overall survival; PDRG1, P53 and DNA damage-regulated gene 1; PFS, progression-free survival; TCGA, The Cancer Genome Atlas. *$P < 0.05$, **$P < 0.01$, ***$P < 0.001$.

Table 1 Clinical features and PDRG1 protein expression in HCC patients

Variable	Number	PDRG1 expression		χ^2	*P*-value
		Low	High		
Sex					
Male	50	25	25		
Female	16	8	8	0	1
Age (year)					
⩽ 50	14	5	9		
> 50	52	28	24	1.451	0.228
PVTT					
No	54	30	24		
Yes	12	3	9	2.546	0.111
Tumor number					
Solitary	52	30	22		
Multiple	14	3	11	4.442	0.035*
Cirrhosis					
No	23	10	13		
Yes	43	23	20	0.601	0.438
Albumin (g/L)					
⩽ 40	20	8	12		
> 40	46	25	21	1.148	0.284
Tumor encapsulation					
No	40	14	26		
Yes	26	19	7	9.138	0.003**
Tumor satellites					
No	45	26	19		
Yes	21	7	14	3.422	0.064
TBIL (μmol/L)					
⩽ 17.1	41	26	15		
> 17.1	25	7	18	7.791	0.005**
Child-pugh					
A	59	31	28		
B	7	2	5	0.639	0.424
ALT (U/L)					
⩽ 40	49	27	22		
> 40	17	6	11	1.981	0.159
AST (U/L)					
⩽ 40	44	26	18		
> 40	22	7	15	4.364	0.037*
Tumor size (cm)					
⩽ 5	48	28	20		
> 5	18	5	13	4.889	0.027*
MVI					
No	35	23	12		
Yes	31	10	21	7.36	0.007**
AFP (ng/mL)					
⩽ 400	58	31	27		
> 400	8	2	6	1.28	0.258
HBsAg					
No	13	7	6		
Yes	53	26	27	0.096	0.757
HBV DNA (U/mL)					
⩽ 10^4	53	27	26		
> 10^4	13	6	7	0.096	0.757

AFP, α-fetoprotein; ALT, alanine transaminase; AST, aspartate transaminase; HBsAg, hepatitis B surface antigen; MVI, microvascular invasion; PDRG1, P53 and DNA damage-regulated gene 1; PVTT, portal vein tumor thrombus; TBIL, total bilirubin. *$P < 0.05$, **$P < 0.01$.

significantly positively correlated with the Wnt/β-catenin and p53 signaling pathways, and negatively correlated with bile acid metabolism in HCC (Fig. 5A). To further substantiate these findings, we constructed a PPI network for PDRG1, which identified RUVBL1, PFDN6, URI1, and UXT as its direct interacting partners (Fig. 5B). Correlation analysis using the GEPIA2 platform in the TCGA-LIHC cohort revealed that among these candidates, RUVBL1 exhibited the strongest positive correlation with PDRG1 mRNA expression (Fig. 5C; Fig. S2A–S2C). Co-immunoprecipitation (Co-IP) assays in Hep3B and PLC/PRF/5 cells confirmed a physical interaction between PDRG1 and RUVBL1 proteins (Fig. 5D). Critically, RUVBL1 has been established as a key regulator that activates the Wnt/β-catenin pathway through chromatin remodeling [21]. Recent evidence demonstrates that RUVBL1-containing complexes can drive the expression of β-catenin and facilitate its nuclear translocation [22]. Therefore, the specific interaction between PDRG1 and RUVBL1 suggests a plausible mechanism whereby PDRG1 may modulate Wnt/β-catenin signaling by engaging this central chromatin regulator. Based on this integrated evidence from GSEA, PPI analysis, and the established role of its binding partner, we focused subsequent investigations on the Wnt/β-catenin pathway.

Western blot analysis confirmed that PDRG1 knockdown for 72 h in Hep3B and PLC/PRF/5 cells significantly decreased the levels of β-catenin, c-Myc, phosphorylated GSK-3β (p-GSK-3β) in the cytoplasm, and nuclear β-catenin (Fig. 5E and 5F). Conversely, PDRG1 overexpression in HCCLM3 cells significantly increased these key Wnt pathway components in both compartments (Fig. 5E and 5F). Collectively, these data, combined with the observed physical interaction between PDRG1 and RUVBL1 and the strong correlation between

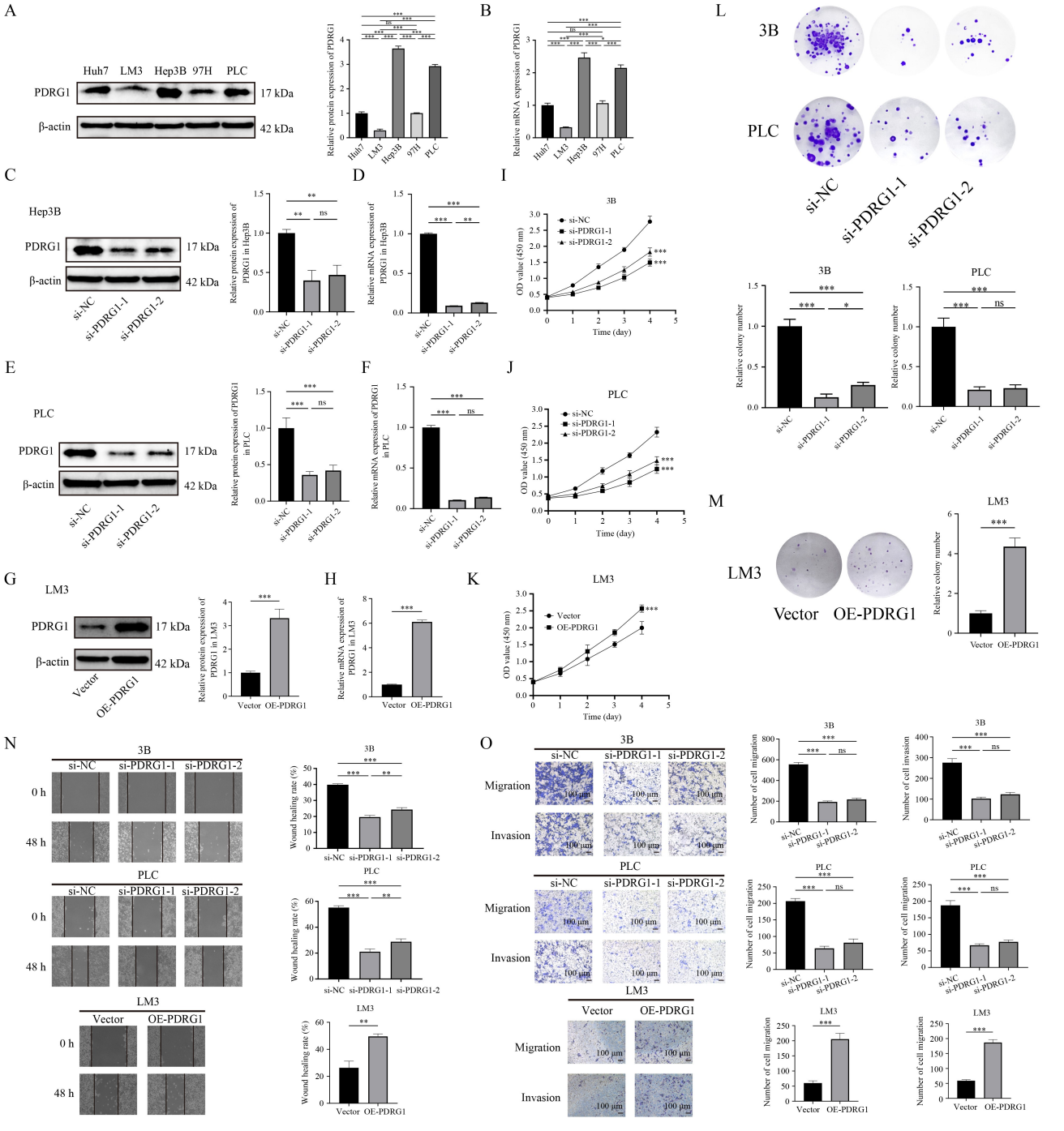

Fig. 3 Effects of PDRG1 knockdown or overexpression on HCC cell proliferation. (A, B) Basal PDRG1 protein (A, Western blot) and mRNA (B, RT-qPCR) expression in five HCC cell lines. (C–F) Efficiency of PDRG1 knockdown in Hep3B (C, D) and PLC/PRF/5 (E, F) cells confirmed by Western blot (C, E) and RT-qPCR (D, F). (G, H) PDRG1 overexpression efficiency in HCCLM3 cells by Western blot (G) and RT-qPCR (H). (I–K) CCK-8 viability assays: PDRG1 knockdown in Hep3B (I) and PLC/PRF/5 (J); overexpression in HCCLM3 (K). (L, M) Colony formation: knockdown in Hep3B/PLC/PRF/5 (L); overexpression in HCCLM3 (M). (N) Wound healing assay for migration. (O) Transwell migration and invasion assays. HCC, hepatocellular carcinoma; OD, optical density; PDRG1, P53 and DNA damage-regulated gene 1. *$P < 0.05$, **$P < 0.01$, ***$P < 0.001$.

PDRG1 expression and Wnt pathway activity, establish PDRG1 as a functional regulator of the Wnt/β-catenin signaling pathway.

XAV939 reverses PDRG1-mediated HCC progression through Wnt/β-catenin pathway inhibition

To determine whether PDRG1 exerts its oncogenic

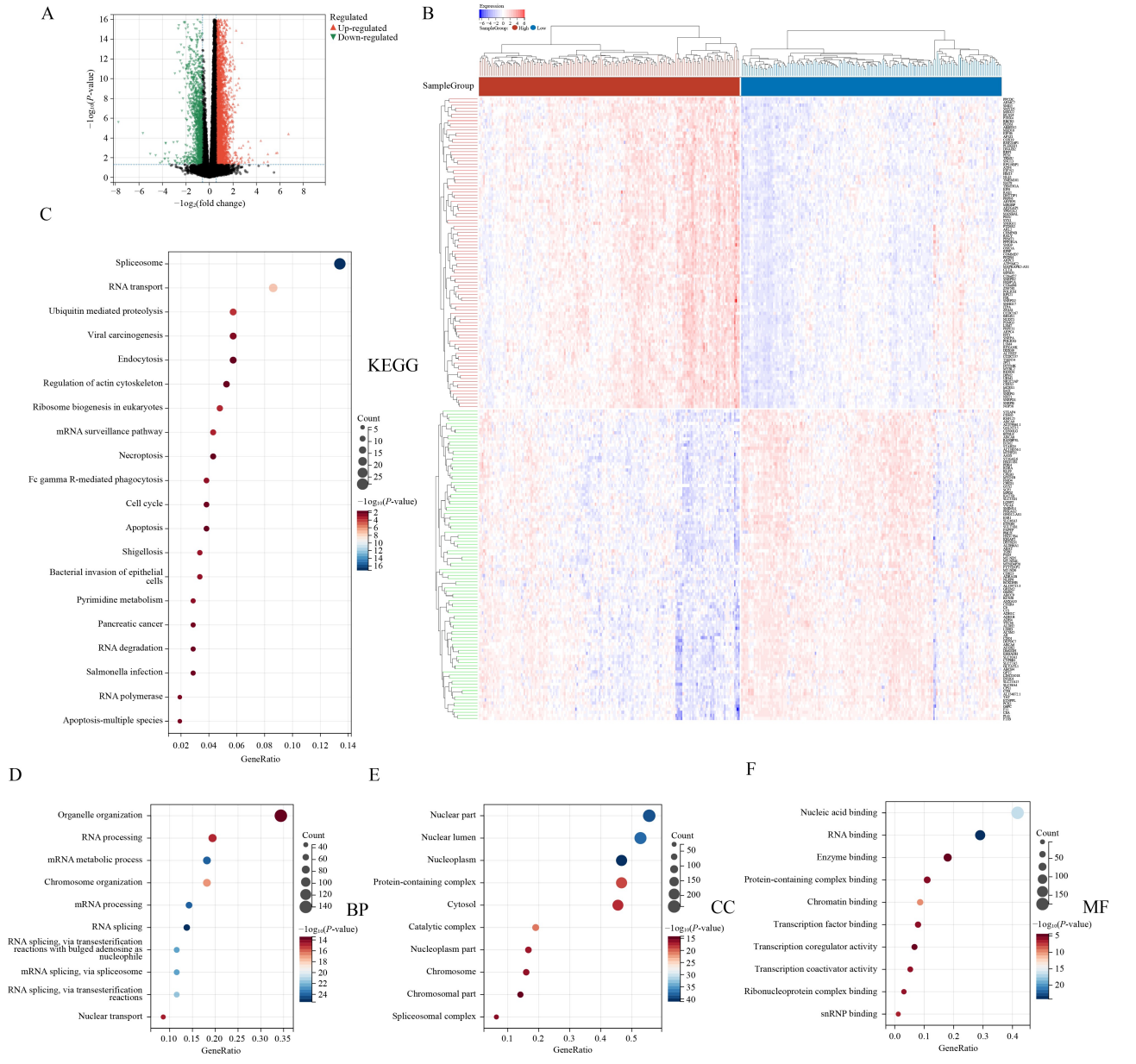

Fig. 4 Transcriptomic profiling identifies DEGs and functional enrichment associated with PDRG1 expression in HCC. (A) Volcano plot of differentially expressed genes (DEGs) between PDRG1-high and PDRG1-low groups in TCGA (red: upregulated; green: downregulated in PDRG1-high). (B) Heatmap of DEGs with clustered expression patterns. (C–F) Enrichment analysis of DEGs: KEGG pathways (C), biological process (D), cellular component (E), and molecular function (F). HCC, hepatocellular carcinoma; PDRG1, P53 and DNA damage-regulated gene 1. *$P < 0.05$, **$P < 0.01$, ***$P < 0.001$.

effects through the Wnt/β-catenin pathway, we performed rescue experiments using the Wnt/β-catenin pathway-specific inhibitor XAV939 (3.5 μmol/L). Overexpression of PDRG1 significantly enhanced HCCLM3 cell proliferation; however, co-treatment with XAV939 completely reversed this pro-proliferative effect (Fig. 6A, 6B, and 6G). Similarly, the enhanced migration and invasion induced by PDRG1 overexpression were also effectively abolished by XAV939 treatment (Fig. 6C–6F).

Extending these observations to *in vivo* settings, we first confirmed in the subcutaneous tumor model that PDRG1 knockdown significantly suppressed Hep3B-derived tumor growth (Fig. 6H). Prior to the lung metastasis experiments, Hep3B cells stably overexpressing PDRG1 were established and validated by both Western blot and RT-qPCR, confirming significantly elevated PDRG1 levels at both protein and mRNA levels ($P < 0.001$) (Fig. 6I). Furthermore, in the lung metastasis model, tail vein injection of OE-PDRG1 Hep3B cells markedly enhanced metastatic burden, which was again substantially attenuated by XAV939 treatment (Fig. 6J).

Collectively, these consistent results from both *in vitro*

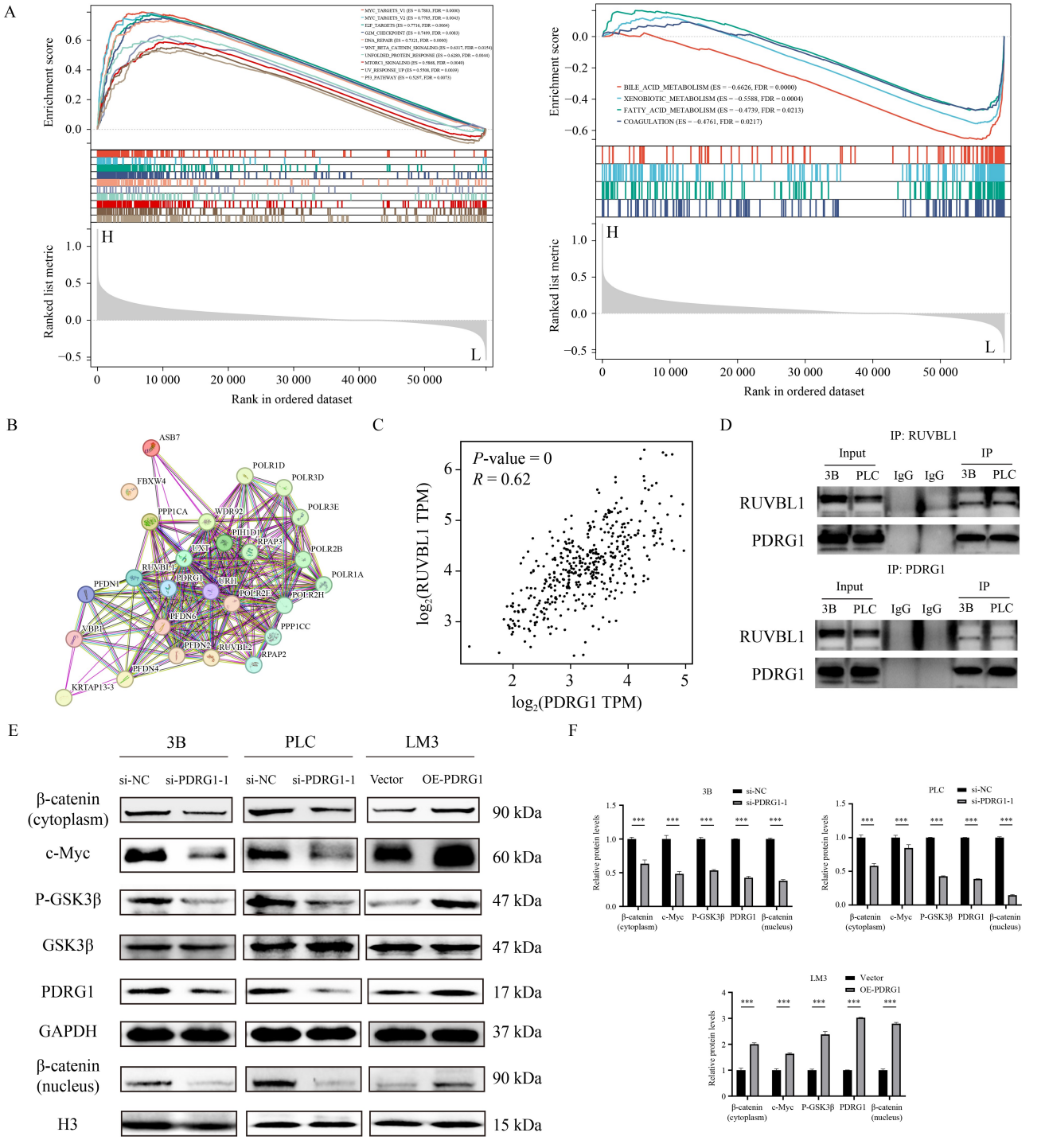

Fig. 5 PDRG1 activates Wnt/β-catenin signaling in HCC. (A) GSEA showing pathways correlated with PDRG1 expression. (B) Protein–protein interaction (PPI) network identifying RUVBL1, PFDN6, URI1, and UXT as direct interacting partners of PDRG1. (C) Correlation analysis between PDRG1 and RUVBL1 mRNA expression in the TCGA-LIHC cohort via GEPIA2. (D) Co-immunoprecipitation (Co-IP) assays confirming physical interaction between PDRG1 and RUVBL1 proteins in Hep3B and PLC/PRF/5 cells. (E, F) Western blot analysis of Wnt/β-catenin pathway proteins in Hep3B/PLC/PRF/5 cells with PDRG1 knockdown (si-PDRG1 vs. si-NC) and HCCLM3 cells with PDRG1 overexpression (OE-PDRG1 vs. vector). HCC, hepatocellular carcinoma; PDRG1, P53 and DNA damage-regulated gene 1. *$P < 0.05$, **$P < 0.01$, ***$P < 0.001$.

and *in vivo* experiments demonstrate that PDRG1 promotes HCC proliferation and metastasis primarily via activation of the Wnt/β-catenin pathway.

SP1 transcriptionally activates PDRG1 by binding its promoter

To identify upstream transcriptional regulators of

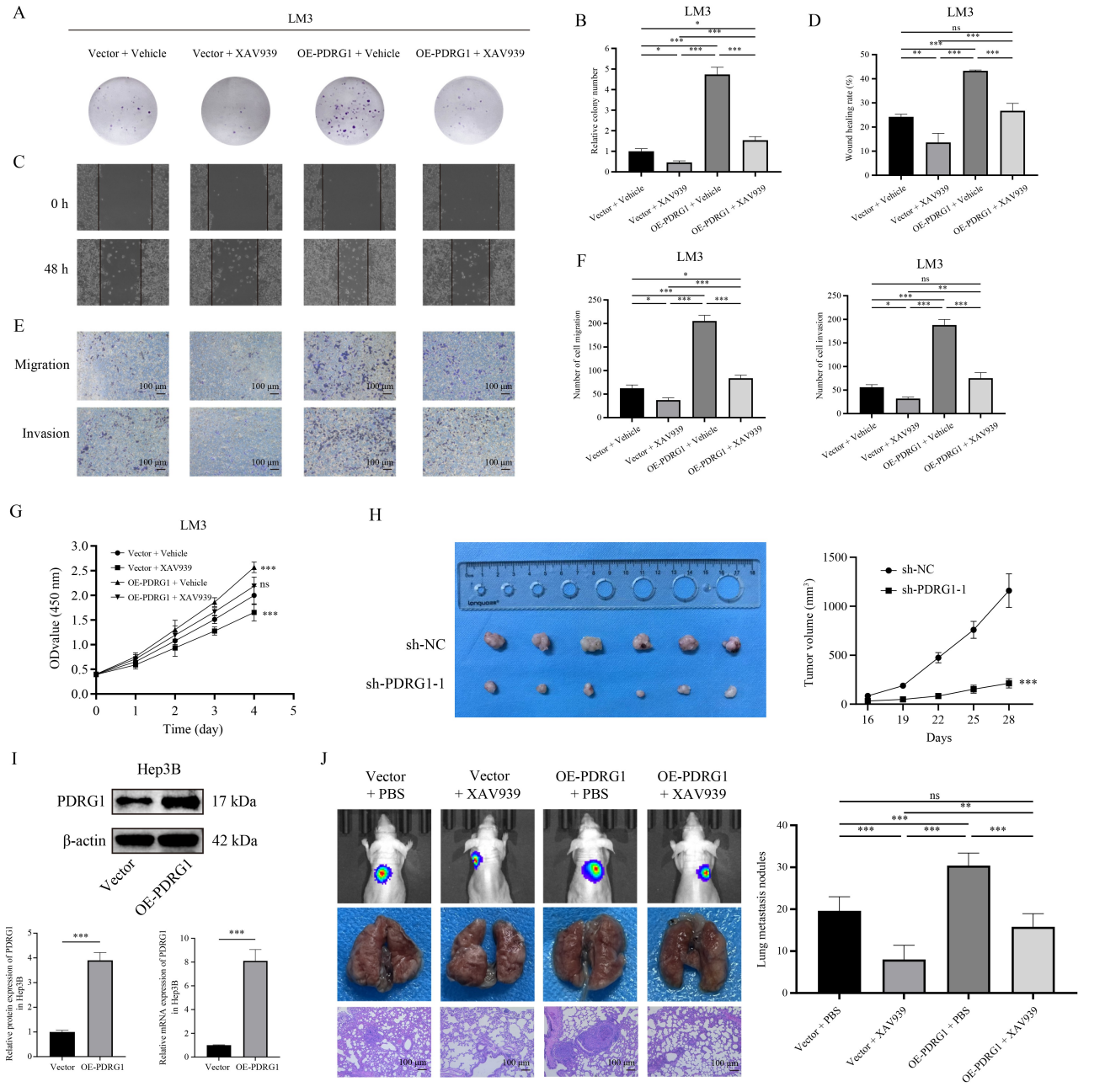

Fig. 6 PDRG1 promotes HCC progression through Wnt/β-catenin signaling *in vitro* and *in vivo*. (A, B) Colony formation assay in HCCLM3 cells transfected with Vector or OE-PDRG1 and treated with Vehicle or XAV939. (C, D) Wound healing assay assessing migration. (E, F) Transwell migration and invasion assays. (G) CCK-8 viability assay in similarly treated HCCLM3 cells. (H) Subcutaneous tumor growth of Hep3B cells with PDRG1 knockdown (shPDRG1-1 vs. shNT). (I) Validation of PDRG1 overexpression in Hep3B cells by Western blot and RT-qPCR. (J) Lung metastasis of OE-PDRG1 Hep3B cells with or without XAV939 treatment, as shown by *in vivo* imaging, representative lung gross images, and H&E staining (100× magnification). HCC, hepatocellular carcinoma; PDRG1, P53 and DNA damage-regulated gene 1. $*P < 0.05$, $**P < 0.01$, $***P < 0.001$.

PDRG1, we intersected predictions from the GTRD, TFDB, PROMO, and KnockTF databases, yielding four candidate transcription factors: CEBPB, SP1, TP53, and MYB. Based on literature review and clinicopathological correlation, SP1 was prioritized for further investigation (Fig. 7A). Analysis of TCGA data via GEPIA2 confirmed a significant positive correlation between SP1 and PDRG1 mRNA expression in HCC tissues ($R = 0.38$, $P = 2.9 \times 10^{-14}$; Fig. 7B). Furthermore, data from TCGA and CPTAC demonstrated significant upregulation of both SP1 mRNA and SP1 protein in HCC tissues compared to adjacent non-tumorous controls (Fig. 7C).

JASPAR database analysis predicted three potential SP1 binding sites within the PDRG1 promoter region: E1

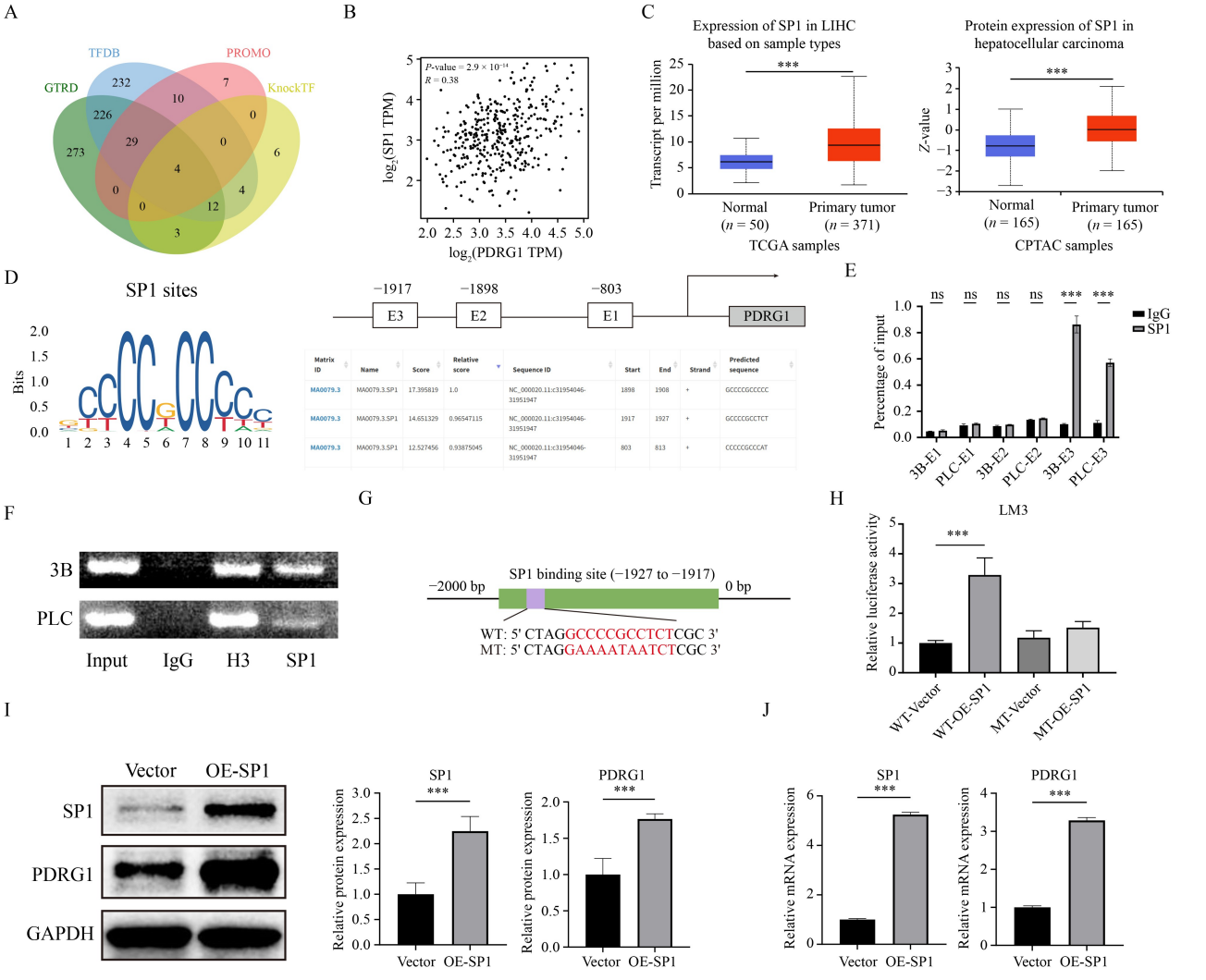

Fig. 7 SP1 transcriptionally activates PDRG1 in HCC. (A) Integrated transcription factor prediction for PDRG1 from multiple databases. (B) Correlation between SP1 and PDRG1 mRNA in TCGA (R = 0.38, $P = 2.9 \times 10^{-14}$). (C) SP1 mRNA (TCGA) and protein (CPTAC) overexpression in HCC versus adjacent tissues. (D) JASPAR-predicted SP1 binding sites in PDRG1 promoter. (E) ChIP-qPCR confirming SP1 binding to E3 site in Hep3B/PLC/PRF/5 cells. (F) Agarose gel electrophoresis of E3 amplicons. (G) E3 wild-type/mutant sequences. (H) Dual-luciferase assay validating SP1-E3 binding in HCCLM3 cells. (I, J) SP1-induced PDRG1 upregulation confirmed by Western blot (I) and RT-qPCR (J) in OE-SP1 HCCLM3 cells. ChIP-qPCR, chromatin immunoprecipitation quantitative PCR; CPTAC, Clinical Proteomic Tumor Analysis Consortium; LIHC, liver hepatocellular carcinoma; PDRG1, P53 and DNA damage-regulated gene 1; TCGA, The Cancer Genome Atlas. *P < 0.05, **P < 0.01, ***P < 0.001.

(−813 to −803), E2 (−1908 to −1898), and E3 (−1927 to −1917) (Fig. 7D). Chromatin Immunoprecipitation qPCR (ChIP-qPCR) in HCC cells confirmed that SP1 specifically bound only to the predicted E3 site (Fig. 7E), validated further by agarose gel electrophoresis (Fig. 7F). Dual-luciferase reporter assays corroborated that SP1 bound to the E3 site, significantly enhancing promoter activity (P < 0.0001, Fig. 7G and 7H). Critically, overexpression of SP1 (OE-SP1) in HCCLM3 cells significantly increased both PDRG1 mRNA and protein levels (P < 0.001, Fig. 7I and 7J). These findings establish SP1 as a direct transcriptional activator of PDRG1.

SP1/PDRG1/Wnt/β-catenin axis promotes HCC malignancy

To investigate whether SP1 regulates the Wnt/β-catenin pathway via PDRG1, we performed rescue experiments assessing Wnt pathway proteins. Overexpression of SP1 increased PDRG1 expression and activated Wnt/β-catenin signaling (elevated β-catenin, c-Myc, p-GSK-3β). Remarkably, this activation was reversed by PDRG1 knockdown (si-PDRG1-1) (Fig. 8A and 8B), demonstrating that SP1 modulates Wnt/β-catenin signaling through PDRG1. Importantly, SP1 overexpression significantly enhanced HCC cell proliferation, migration, and invasion.

Co-treatment with si-PDRG1-1 effectively reversed these SP1-induced oncogenic phenotypes (Fig. 8C–8I).

Complementary rescue experiments were performed to further validate this regulatory hierarchy. SP1 knockdown suppressed both PDRG1 expression and Wnt/β-catenin signaling activation (Fig. 9A and 9B), whereas concurrent PDRG1 overexpression effectively restored pathway activity (Fig. 9C–9I). These results conclusively demonstrate that the SP1/PDRG1/Wnt/β-catenin signaling axis promotes the proliferation, migration, and invasion of HCC cells.

Discussion

PDRG1 has been implicated in the pathogenesis of diverse malignancies, including testicular, liver, cervical, lung, ovarian, and gastric cancers [23]. Since its initial discovery in 2003 as a gene regulated by UV radiation and p53 [5], subsequent research has focused on elucidating its molecular mechanisms and associated signaling pathways in both neoplastic and non-neoplastic tissues [24–26]. In this study, *in silico* analyses revealed significantly elevated PDRG1 mRNA and protein expression in HCC tissues compared to adjacent non-tumorous liver. Critically, high PDRG1 mRNA expression correlated positively with advanced tumor stage and grade, and negatively with OS, DSS, DFS, and PFS in HCC patients. These findings were validated experimentally: Western blot and RT-qPCR analyses of 66 paired HCC and adjacent normal tissues confirmed PDRG1 overexpression in tumors. IHC analysis on a subset of 30 paired samples further corroborated this, and subgroup analysis established significant associations between elevated PDRG1 protein expression and adverse

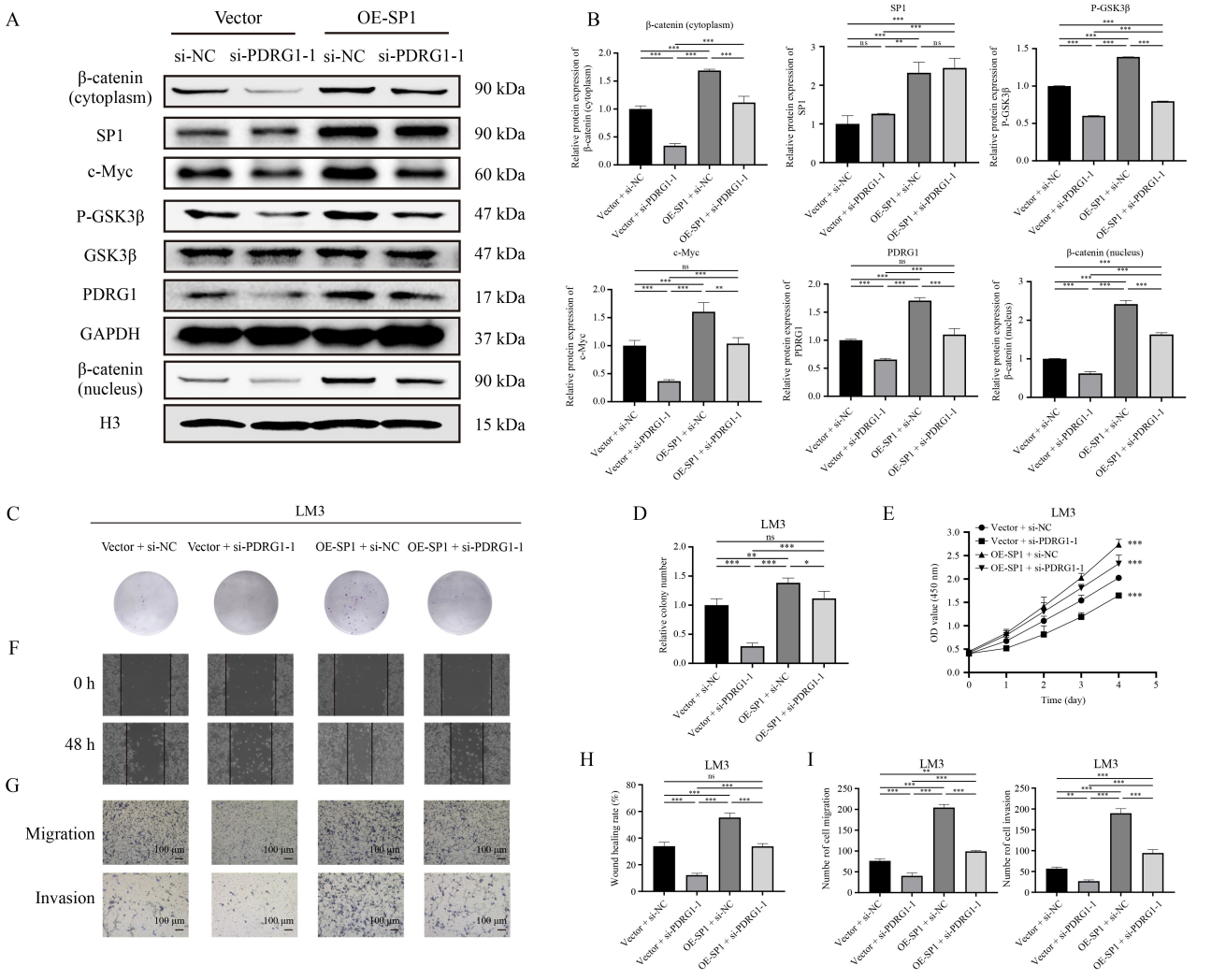

Fig. 8 SP1 activates Wnt/β-catenin signaling through PDRG1 in HCC cells. (A, B) Western blot analysis of Wnt/β-catenin pathway proteins in HCCLM3 rescue experiments: SP1 overexpression with/without PDRG1 knockdown. (C, D) Colony formation assay under corresponding conditions. (E) CCK-8 viability assay. (F, H) Wound healing migration assay. (G, I) Transwell migration and invasion assays. HCC, hepatocellular carcinoma; PDRG1, P53 and DNA damage-regulated gene 1. *$P < 0.05$, **$P < 0.01$, ***$P < 0.001$.

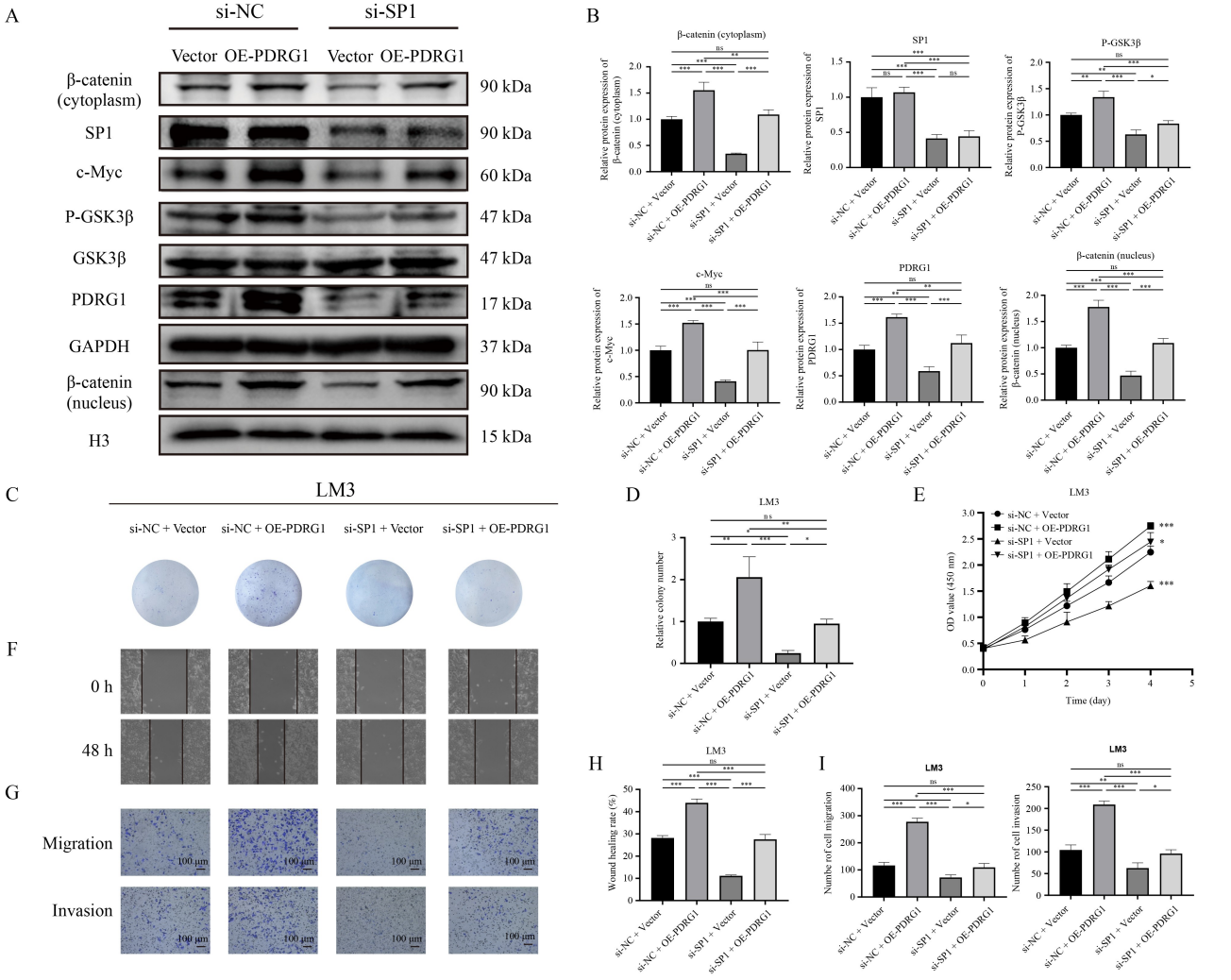

Fig. 9 PDRG1 overexpression rescues Wnt/β-catenin signaling impaired by SP1 knockdown. (A, B) Western blot analysis of Wnt/β-catenin pathway proteins in HCCLM3 cells with SP1 knockdown and/or PDRG1 overexpression. (C, D) Colony formation assay under corresponding conditions. (E) CCK-8 viability assay. (F, H) Wound healing migration assay. (G, I) Transwell migration and invasion assays. HCC, hepatocellular carcinoma; PDRG1, P53 and DNA damage-regulated gene 1. *$P < 0.05$, **$P < 0.01$, ***$P < 0.001$.

clinicopathological parameters, including increased tumor number, capsular invasion, larger tumor diameter, higher incidence of MVI, and elevated aspartate aminotransferase (AST) levels. Notably, PDRG1 expression showed no significant correlation with gender, age, portal vein tumor thrombus, or liver cirrhosis. Collectively, these results provide compelling evidence that PDRG1 is overexpressed in HCC and associated with poor prognosis. This prompted our investigation into the biological functions and molecular mechanisms of PDRG1 in HCC pathogenesis.

Recent studies support PDRG1's oncogenic role: it is overexpressed in colorectal cancer and promotes malignant progression via the p21-mediated signaling pathway [7]. Similarly, PDRG1 has been linked to Wnt signaling activation in esophageal cancer [9]. While our study confirms PDRG1 overexpression in human HCC, its specific biological functions and mechanisms in this context remain incompletely defined. To address this, we established PDRG1 gain-of-function (OE-PDRG1) and loss-of-function (si-PDRG1 and si-PDRG1-2) HCC cell models. Our functional assays demonstrated that PDRG1 knockdown significantly suppressed HCC cell proliferation, migration, and invasion. To investigate the underlying mechanism, we hypothesized that PDRG1 might regulate the Wnt/β-catenin pathway. This hypothesis was based on two key lines of predictive evidence. First, our PPI analysis revealed that PDRG1 physically binds to RUVBL1, a known chromatin remodeling ATPase. Importantly, RUVBL1 has been established as a direct activator of the Wnt/β-catenin pathway in cancer. Critically, RUVBL1 is a key regulator that activates the Wnt/β-catenin pathway through chromatin remodeling [21], and recent evidence demonstrates that RUVBL1-containing complexes can drive the expression of β-catenin and facilitate its nuclear

translocation [22]. Second, GSEA indicated a significant positive correlation between PDRG1 expression and Wnt/β-catenin signaling activity in HCC. To experimentally test this hypothesis, we examined the core components of the Wnt pathway. Mechanistically, and consistent with our prediction, PDRG1 depletion downregulated key Wnt/β-catenin pathway components, including p-GSK-3β and β-catenin. Conversely, PDRG1 overexpression enhanced these malignant phenotypes and activated Wnt signaling by upregulating the same components. Crucially, rescue experiments using the specific Wnt/β-catenin pathway inhibitor XAV939 reversed the pro-proliferative and pro-metastatic effects induced by PDRG1 overexpression in both *in vitro* and *in vivo* settings. These data provide robust evidence that PDRG1 acts as an oncogene in HCC, primarily mediated through Wnt/β-catenin signaling, and identify it as a potential therapeutic target.

While previous studies described PDRG1's association with cancer and its downstream signaling [27,28], the upstream transcriptional regulators of PDRG1 remained unexplored. Our study is the first to report that the transcription factor SP1 binds to the PDRG1 promoter and directly activates its transcription. SP1 is a well-established transcription factor implicated in diverse cancers, regulating the transcription of numerous genes critical for tumorigenesis [29–31]. For instance, SP1 promotes lung cancer growth by transcriptionally activating MALAT1 [32] and facilitates gastric cancer progression by enhancing PD-L1 transcription [33]. Our preliminary findings indicated SP1-mediated upregulation of PDRG1 expression. Dual-luciferase reporter assays identified the specific binding site E3 (−1927 to −1917) within the PDRG1 promoter responsible for SP1 binding. Furthermore, rescue experiments demonstrated that the SP1/PDRG1/Wnt/β-catenin signaling axis regulates the proliferation, migration, and invasion of HCC cells. These novel discoveries highlight the SP1/PDRG1 axis as a promising therapeutic target for HCC.

Our study has several limitations. First, the detailed molecular interplay between SP1 and PDRG1 in HCC, particularly concerning potential epigenetic modifications (e.g., histone acetylation/methylation), warrants further investigation. Second, due to technical constraints, we were unable to perform double immunofluorescence staining to precisely co-localize SP1 and PDRG1 expression within tumor tissues. Finally, *in vivo* rescue experiments validating whether SP1 promotes HCC proliferation, metastasis, and invasion specifically through PDRG1 are necessary to fully establish the translational relevance of this axis.

In summary, our study identifies PDRG1 as an oncogenic driver in HCC, where its overexpression correlates with advanced tumor progression and poor prognosis. Mechanistically, PDRG1 activates Wnt/β-catenin signaling to promote HCC proliferation, migration, and invasion. We further demonstrate that SP1 transcriptionally upregulates PDRG1 by binding to its promoter, forming a novel SP1/PDRG1/Wnt/β-catenin axis that drives HCC malignancy. Rescue experiments confirm the therapeutic potential of targeting this pathway. These findings establish the SP1-PDRG1-Wnt/β-catenin axis as a promising therapeutic target for the treatment of HCC.

Acknowledgements

This work was supported by National Natural Science Foundation of China (Nos. 82472743, 82300921, and 82573164); Development of a Precision Management System for Biliary Tract Tumors (No. SC2024ZX12C0024); Heilongjiang Provincial Natural Science Foundation of China (No. PL2024H115); Guangxi Science and Technology Program (No. AD25069077); Natural Science Foundation of Heilongjiang Province (No. LH2023H043); Open Funds of State Key Laboratory of Oncology in South China (No. HN2025-02); Open Funds of Shanghai Key Laboratory of Cancer Systems Regulation and Clinical Translation (No. CSRCT-KF0002); Open Research Project from Key Laboratory of Clinical Laboratory Medicine of Guangxi Department of Education (No. GXGXLCJYZDX2025001); Guangxi Science and Technology Program (No. AD25069077); Open Research Fund of Key Laboratory of Gastrointestinal Cancer (Fujian Medical University), Ministry of Education (No. FMUGIC-202501); Open Funds of Key Laboratory of Clinical Laboratory Technology for Precision Medicine (No. FKLCLT-202504); Open Research Fund of Anhui Province Key Laboratory of Non-coding RNA Basic and Clinical Transformation (No. NcRNA202508); Thematic Research Support Scheme of State Key Laboratory of Liver Research, The University of Hong Kong (No. SKLLR/TRSS/2025/08).

Compliance with ethics guidelines

Conflicts of interest Xudong Zhao, Shihua Lv, Haikuan Wang, Zeyi Lu, Pengcheng Kang, Jinglin Li, Liang Yu, Shihui Ma, Changxing Hua, Junqi You, Ziqiang Ge, Yi Xu, and Yunfu Cui declare that they have no conflict of interest.

This study was approved by the Ethics Committee of the Second Affiliated Hospital of Harbin Medical University (Approval No. YSJKY2024-235) and was performed in accordance with the ethical standards as laid down in the 1964 Declaration of Helsinki and its later amendments or comparable ethical standards. Written informed consent was obtained from all participants, and all animal procedures followed the institutional and national guidelines for the care and use of laboratory animals.

Data availability and compliance statement

The authors declare that the acquisition and subsequent use of all data presented in this manuscript comply fully with all relevant

local, national, and international laws, regulations, ethical guidelines, and the terms of use associated with the original data sources.

The authors bear full legal responsibility for ensuring the legality of data acquisition and all subsequent uses.

All data generated or analyzed during this study, which support the findings of this study, are available from the corresponding author on reasonable request. To request access to the data, please contact Dr. Xudong Zhao.

Electronic supplementary material Supplementary material is available in the online version of this article at https://doi.org/10.1007/s11684-026-1237-8 and is accessible for authorized users.

References

1. Sung H, Ferlay J, Siegel RL, Laversanne M, Soerjomataram I, Jemal A, Bray F. Global cancer statistics 2020: GLOBOCAN estimates of incidence and mortality worldwide for 36 cancers in 185 countries. CA Cancer J Clin 2021; 71(3): 209–249
2. Llovet JM, Kelley RK, Villanueva A, Singal AG, Pikarsky E, Roayaie S, Lencioni R, Koike K, Zucman-Rossi J, Finn RS. Hepatocellular carcinoma. Nat Rev Dis Primers 2021; 7(1): 6
3. Rebouissou S, Nault JC. Advances in molecular classification and precision oncology in hepatocellular carcinoma. J Hepatol 2020; 72(2): 215–229
4. Vogel A, Meyer T, Sapisochin G, Salem R, Saborowski A. Hepatocellular carcinoma. Lancet 2022; 400(10360): 1345–1362
5. Luo X, Huang Y, Sheikh MS. Cloning and characterization of a novel gene PDRG that is differentially regulated by p53 and ultraviolet radiation. Oncogene 2003; 22(46): 7247–7257
6. Pajares M. PDRG1 at the interface between intermediary metabolism and oncogenesis. World J Biol Chem 2017; 8(4): 175–186
7. Xu Y, Liu J, Jiang T, Shi L, Shang L, Song J, Li L. PDRG1 predicts a poor prognosis and facilitates the proliferation and metastasis of colorectal cancer. Exp Cell Res 2021; 409(2): 112924
8. Zhang YJ, Li JQ, Li HZ, Song H, Wei CS, Zhang SQ. PDRG1 gene silencing contributes to inhibit the growth and induce apoptosis of gastric cancer cells. Pathol Res Pract 2019; 215(10): 152567
9. Tao Z, Zhang Y, Zhu S, Ni Z, You Q, Sun X, Xu D. Knockdown of PDRG1 could inhibit the Wnt signaling pathway in esophageal cancer cells. Ann Clin Lab Sci 2019; 49(6): 794–803
10. Pećina-Šlaus N. Wnt signal transduction pathway and apoptosis: a review. Cancer Cell Int 2010; 10(1): 22
11. Khalaf AM, Fuentes D, Morshid AI, Burke MR, Kaseb AO, Hassan M, Hazle JD, Elsayes KM. Role of Wnt/β-catenin signaling in hepatocellular carcinoma, pathogenesis, and clinical significance. J Hepatocell Carcinoma 2018; 5: 61–73
12. Liu J, Xiao Q, Xiao J, Niu C, Li Y, Zhang X, Zhou Z, Shu G, Yin G. Wnt/β-catenin signalling: function, biological mechanisms, and therapeutic opportunities. Signal Transduct Target Ther 2022; 7(1): 3
13. Katoh M. Canonical and non-canonical WNT signaling in cancer stem cells and their niches: cellular heterogeneity, omics reprogramming, targeted therapy and tumor plasticity. Int J Oncol 2017; 51(5): 1357–1369
14. Neiheisel A, Kaur M, Ma N, Havard P, Shenoy AK. Wnt pathway modulators in cancer therapeutics: an update on completed and ongoing clinical trials. Int J Cancer 2022; 150(5): 727–740
15. Song P, Gao Z, Bao Y, Chen L, Huang Y, Liu Y, Dong Q, Wei X. Wnt/β-catenin signaling pathway in carcinogenesis and cancer therapy. J Hematol Oncol 2024; 17(1): 46
16. Briggs MR, Kadonaga JT, Bell SP, Tjian R. Purification and biochemical characterization of the promoter-specific transcription factor, Sp1. Science 1986; 234(4772): 47–52
17. Vizcaíno C, Mansilla S, Portugal J. Sp1 transcription factor: a long-standing target in cancer chemotherapy. Pharmacol Ther 2015; 152: 111–124
18. Beishline K, Azizkhan-Clifford J. Sp1 and the 'hallmarks of cancer'. FEBS J 2015; 282(2): 224–258
19. Safe S, Imanirad P, Sreevalsan S, Nair V, Jutooru I. Transcription factor Sp1, also known as specificity protein 1 as a therapeutic target. Expert Opin Ther Targets 2014; 18(7): 759–769
20. O'Connor L, Gilmour J, Bonifer C. The role of the ubiquitously expressed transcription factor Sp1 in tissue-specific transcriptional regulation and in disease. Yale J Biol Med 2016; 89(4): 513–525
21. Feng Y, Lee N, Fearon ER. TIP49 regulates beta-catenin-mediated neoplastic transformation and T-cell factor target gene induction via effects on chromatin remodeling. Cancer Res 2003; 63(24): 8726–8734
22. Zhang Z, Gao Y, Qian Y, Wei B, Jiang K, Sun Z, Zhang F, Yang M, Baldi S, Yu X, Zuo Y, Ren S. The Lyn/RUVBL1 complex promotes colorectal cancer liver metastasis by regulating arachidonic acid metabolism through chromatin remodeling. Adv Sci (Weinh) 2025; 12(5): e2406562
23. Liu Z, Huang K, He Y, Hao S, Wei Z, Peng T. A pan-cancer analysis of the expression and prognostic significance of PDRG1. Ann Transl Med 2023; 11(2): 36
24. Zhang W, Yao F, Zhang H, Li N, Zou X, Sui L, Hou L. The potential roles of the apoptosis-related protein PDRG1 in diapause embryo restarting of Artemia sinica. Int J Mol Sci 2018; 19(1): 126
25. Sun J, Xu Y, Liu J, Cui H, Cao H, Ren J. PDRG1 promotes the proliferation and migration of GBM cells by the MEK/ERK/CD44 pathway. Cancer Sci 2022; 113(2): 500–516
26. Xu T, Xiao D. Oleuropein enhances radiation sensitivity of

nasopharyngeal carcinoma by downregulating PDRG1 through HIF1α-repressed microRNA-519d. J Exp Clin Cancer Res 2017; 36(1): 3

27. Tao Z, Chen S, Mao G, Xia H, Huang H, Ma H. The PDRG1 is an oncogene in lung cancer cells, promoting radioresistance via the ATM-P53 signaling pathway. Biomed Pharmacother 2016; 83: 1471–1477
28. Gu Z, Wu S, Wang J, Zhao S. Long non-coding RNA LINC01419 mediates miR-519a-3p/PDRG1 axis to promote cell progression in osteosarcoma. Cancer Cell Int 2020; 20(1): 147
29. Black AR, Black JD, Azizkhan-Clifford J. Sp1 and krüppel-like factor family of transcription factors in cell growth regulation and cancer. J Cell Physiol 2001; 188(2): 143–160
30. Sun X, Xiao C, Wang X, Wu S, Yang Z, Sui B, Song Y. Role of post-translational modifications of Sp1 in cancer: state of the art. Front Cell Dev Biol 2024; 12: 1412461
31. Safe S. Specificity proteins (Sp) and cancer. Int J Mol Sci 2023; 24(6): 5164
32. Li S, Wang Q, Qiang Q, Shan H, Shi M, Chen B, Zhao S, Yuan L. Sp1-mediated transcriptional regulation of MALAT1 plays a critical role in tumor. J Cancer Res Clin Oncol 2015; 141(11): 1909–1920
33. Tao LH, Zhou XR, Li FC, Chen Q, Meng FY, Mao Y, Li R, Hua D, Zhang HJ, Wang WP, Chen WC. A polymorphism in the promoter region of PD-L1 serves as a binding-site for SP1 and is associated with PD-L1 overexpression and increased occurrence of gastric cancer. Cancer Immunol Immunother 2017; 66(3): 309–318